

Corrosion Protection of Carbon Steel in Neutral Medium using *Citrus medica* [CM] leaf as an Inhibitor

J. Yamuna*, Noreen Anthony

Department of Chemistry, Holy Cross College (Autonomous), Tiruchirappalli 620002, Tamil Nadu, India

Abstract: The effect of *Citrus medica* leaf on the corrosion of carbon steel in neutral medium has been studied by mass loss measurements at different time. The present investigation revealed that the percentage of inhibition efficiency is increased with increase of inhibitor concentration and decreased with rise in period of contact. The corrosion products on the metal surface in the presence and absence of inhibitor is analysed by FTIR and UV studies. The observed results concluded that the CM leaf could serve as an effective inhibitor on carbon steel in neutral medium environment.

Keywords : *Citrus medica*, Mass loss, Carbon steel, FTIR.

1. Introduction

The study of corrosion inhibition of mild steel using green inhibitor, is one of the challenging topic of current research in various industries involving chemical cleaning, descaling, pickling, acid oil-well acidizing, etc. [1-3]. A new generation of corrosion inhibitors based on dispersed nanoparticles and nanocomposites can be used as dispersed phase or in smart organic coatings for steel [4-6]. These materials named as nanocontainers that can respond quickly to changes in the corrosive environment. The electrochemical behavior of corrosion inhibitors encapsulated within nanocontainers was triggered by the corrosion process to inhibit these environments [7-9]. Moreover, these materials have superior properties such as antibacterial, anticorrosion and antistatic. One of the disadvantages of these materials is the direct introduction of inhibitor components into protective coatings very often which leads to the degradation and deactivation of a corrosion inhibitor and of the polymer matrix [10]. To overcome this limitation, the complexation of organic molecules by cyclodextrin [11] or the use of oxide nanoparticles, which can play the role of nanocarriers for corrosion inhibitors adsorbed on their surface. The design of these materials is based on the core-shell structure in which the nanocontainers should have good compatibility with the matrix components. Moreover, a shell should have permeability properties that can be controlled by external stimuli.

2. Experimental

2.1. Preparation of extract

The flowers were collected, shade dried and powdered. Plant materials are dried in shade so as to enrich the active principles in them, by reducing their moisture content. The extract was prepared by refluxing 50 g of powdered dry leaves in 500 mL of ethanol for 12 h. The extract and solvent was separated using distillation process. The pure extract was made up to 100 mL and this was taken as stock solution.

2.2. Preparation of specimens

Rectangular samples of area 4x1 cm² have been cut from a large sheet of mild steel. The samples were polished, drilled a hole at one end and numbered by punching. During the study the samples were polished with 400 grade emery papers, degreased in a solution of non-toxic detergent, washed with distilled water, dried, weighed and stored in desiccators for further use.

2.3. Weight loss method

Carbon steel specimens in triplicate were immersed in 100 ml of the solutions containing various concentrations of the inhibitor for one day. The weight of the specimens before and after immersion were determined using Shimadzu balance, model AY 62. The corrosion products were cleansed with Clarke's solution [15]. The inhibition efficiency (IE) was then calculated using the equation;

$$IE = 100 [1 - (W_2/W_1)] \% \quad (1)$$

where W_1 is the corrosion rate in the absence of the inhibitor, W_2 is the corrosion rate in the presence of the inhibitor.

2.4. Potentiodynamic polarization measurement

Potentiodynamic polarisation studies were carried out using VSP primeton. 100 ml of DD water without and with 300 ppm of the inhibitor was taken in an electrochemical cell. The polished electrode was then introduced. The electrode was placed at 0.8 mV to its open circuit potential. Thus the potential was scanned at 10 mV/sec towards the anodic direction in Tafel extrapolation. Applied potential vs. current was plotted and on extrapolation of linear portion to the corrosion potential gives the corrosion current. In anodic and cathodic plot, the slope of the linear portion gives Tafel constants ' b_a ' and ' b_c ' respectively. According to the Stern-Geary equation, the steps of the linear polarization plot are substituted to get corrosion current.

$$I_{corr} = \frac{b_a \times b_c}{2.3(b_a + b_c)R_p}$$

Where, R_p is polarization resistance.

2.5. AC Impedance studies

Impedance measurements were carried out at various corrosion potentials. An ac sine wave of 10 mV amplitude was applied to the electrode. The frequency which is varied from 10 KHz to 100 MHz was superimposed at the open circuit potential. The results are presented in the form of Nyquist plot. All the measurements were presented in the corrosion potential. In Impedance method, the charge transfer resistance (R_{ct}) is obtained from the plots of Z' vs. Z'' (real part Vs imaginary part; Nyquist plot). The value ($R_p + R_s$) corresponds to the point where the plot cuts Z axis to the point where the semicircle cuts the Z axis at high frequency. The difference gives the R_p values, which were substituted in the Stern-Geary equation to get

$$I_{corr} = \frac{b_a \times b_c}{2.3(b_a + b_c)R_{ct}}$$

The b_a and b_c values were experimentally obtained.

2.6. FTIR Spectroscopy

The FTIR spectra of pure *Citrus medica* and (b) thin film formed on the surface of the carbon steel immersed in DD water containing *Citrus medica* was recorded using FTIR.

2.7. UV-Vis spectroscopy

The UV-vis spectroscopy of Mn^{2+} , Fe^{2+} ion, *Citrus medica*, *Citrus medica*+ Mn^{2+} , and *Citrus medica* + Fe^{2+} ion is measured.

3. Results and Discussion

3.1. Mass loss studies

The inhibitor was tested for six different concentrations and their corresponding weight loss data are presented in Table 1 (Figs. 1 and 2). The addition of inhibitors increases the IE, irrespective of the time of immersion. This may be due to the adsorption of phytochemical constituents of the extracts on the metal surface. The IE is 81.58% at a concentration of 300 ppm. The results concerned with the effect of period of immersion at various concentrations of the inhibitors on mild steel in DD water are also shown in Table 2. The IE increases from 81.5% to 95.8% from the first day to the seventh day, on the fifteenth and thirtieth day, the IE found to be only 60.3% and 52.1%. The decrease in IE with time may be attributed to various factors such as an increase in the ferrous ion concentration.

Table 1. Corrosion rates of carbon steel in DD water in the presence and absence of the inhibitor system and the inhibition efficiencies obtained by the mass-loss method.

Inhibitor system: CM + Mn²⁺

S.No	CM (ppm)	Mn ²⁺ (ppm)	Corrosion Rate (mdd)	Inhibition Efficiency (%)
1	0	0	38	-
2	0	20	28.5	25
3	100	20	22.6	40.52
4	200	20	21.2	44.2
5	300	20	7.0	81.58
6	400	20	6.99	81.60
7	500	20	6.99	81.60
8	600	20	6.92	81.79

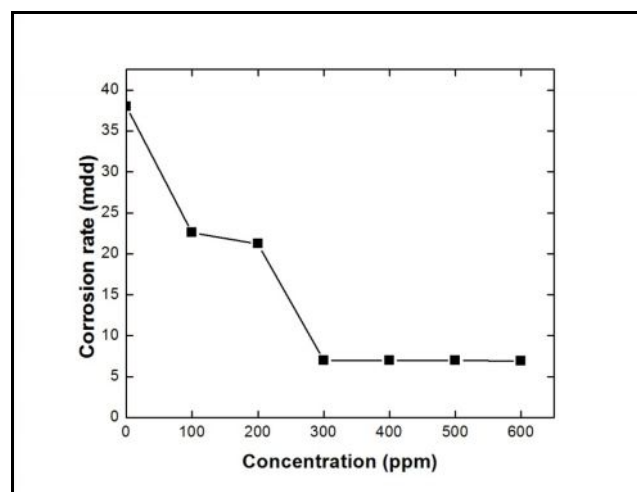


Fig. 1. Corrosion rate of carbon steel in DD water by CM + Mn²⁺ system

Table 2. Effect of duration of immersion on the IE of CM + Mn²⁺ system. Corrosion rates of carbon steel in DD water in the presence and absence of the inhibitor system and the inhibition efficiencies obtained by the mass-loss method.

Inhibitor System: CM + Mn²⁺

S.No	CM (ppm)	Mn ²⁺ (ppm)	Immersion period (days)	Corrosion Rate (mdd)	Inhibition Efficiency (%)
1	300	20	1	7.0	81.58
2	300	20	3	9.6	89.34
3	300	20	5	5.9	95.8
4	300	20	7	9.5	95.2
5	300	20	15	15.1	60.3
6	300	20	30	18.2	52.1

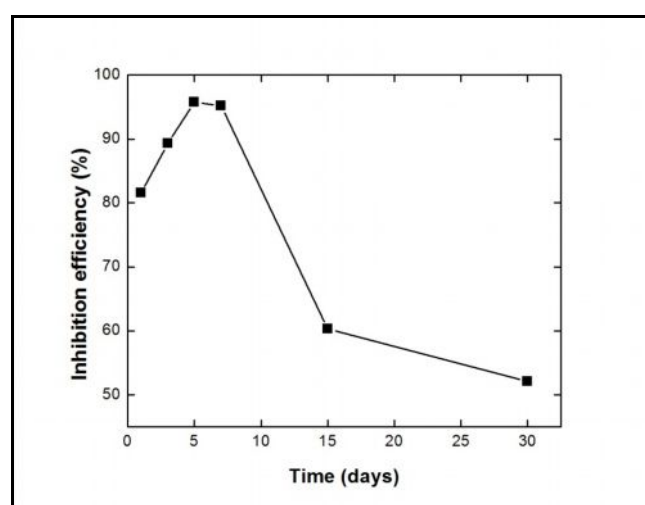


Fig. 2. Effect of duration of immersion on the CR of carbon steel CM+Mn²⁺ system

3.2. Potentiodynamic polarization results

The various electrochemical parameters calculated from Tafel plot (Fig. 3) are given in Table 3. The lower corrosion current density (I_{corr}) values in the presence of inhibitor without causing significant changes in corrosion potential (E_{corr}) (-519 to -478 mV suggests that the compound is mixed type inhibitor (i.e., inhibit both anodic and cathodic reactions) and are adsorbed on the surface thereby blocking the corrosion reaction. Since b_c is greater than b_a suggesting that though the inhibition is under mixed control, the effect of the inhibitor on the cathodic polarization is more pronounced than on the anodic polarization.

- (a) Tafel plot for mild steel in DD water.
 (b) Tafel plot for mild steel in DD water with CM.

Table 3. Results of potentiodynamic polarization studies

Medium: DD water

Inhibitor system: CM (300 ppm) + Mn²⁺ (20 ppm)

S. No	Environment	E_{corr} (mV vs SCE)	b_a (mV)	b_c (mV)	R_p (Ω cm ²)	I_{corr} (A/cm ²)
1	DD water	-519	101.2	273.24	3.14×10^5	1.0218×10^{-4}
2	Inhibitor system in DD water	-478	160.77	306	7.65×10^5	5.9879×10^{-5}

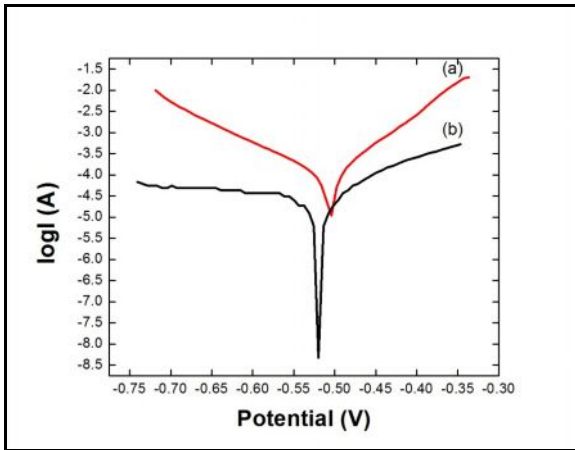


Fig. 3. Results of Potentiodynamic polarisation curves of carbon steel

Medium: DD water

Inhibitor: CM (300 ppm)

(a) DD water

(b) CM (300 ppm) + Mn²⁺ (20 ppm) in DD water

3.3. Electrochemical impedance spectroscopy results

Impedance diagram (Nyquist plot) obtained for mild steel DD water in the presence of various concentrations of the inhibitor is depicted in Fig. 4. They are perfect semicircles and this was attributed to charge transfer reaction. Impedance parameters derived from Nyquist plots are tabulated in Table 4. It can be seen that the resistance has increased and C_{dl} values has decreased. Decrease in C_{dl}, which can result from an increase in thickness of electrical double layer, suggests that the inhibitor molecules function by adsorption at the metal-solution interface.

Table 3. Results of AC impedance studies

Medium: DD water

Inhibitor System: CM + Mn²⁺

S.No	Environment	CM (ppm)	Mn ²⁺ (ppm)	R _{ct} (Ω cm ²)	C _{dl} (F/cm ²)
1	DD water	0	0	7.624×10 ⁶	3.317×10 ⁻¹⁰
2	Inhibitor system in DD water	300	20	5.684×10 ⁷	2.964×10 ⁻¹⁰

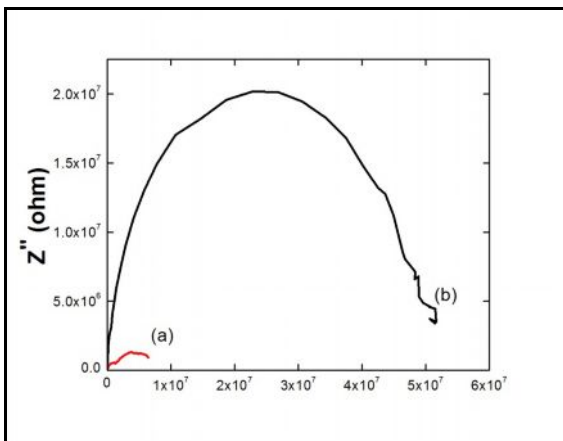


Fig. 4. AC impedance of carbon steel immersed in various environments

Medium: DD water

Inhibitor: CM (300 ppm)

(a) DD water

(b) CM (300 ppm) + Mn²⁺ (20 ppm) in DD water

3.4. Analysis of FTIR spectra

The FTIR spectrum of the pure extract is shown in Fig. 5a. The band at 3439 cm^{-1} is due to the presence of $-\text{OH}$. The lowering of the $-\text{OH}$ stretching frequency. The bands at 1638 cm^{-1} and 1390 cm^{-1} are due to the coupling of $-\text{C}-\text{O}$ stretching and $-\text{C}-\text{O}-\text{H}$ in-plane bending vibration. The bands at 1056 cm^{-1} and 882 cm^{-1} are due to $-\text{C}-\text{O}$ ring vibration.

Figure 5b shows the FTIR spectrum of carbon steel immersed in the presence of the extract. The $-\text{OH}$ frequency of the extract at 3439 cm^{-1} is shifted to 3443 cm^{-1} . The bands at 1638 cm^{-1} and 1390 cm^{-1} which are due to the coupling of $-\text{C}-\text{O}$ stretching and $-\text{C}-\text{O}-\text{H}$ in-plane bending of the carboxylate anion are shifted to 1640 cm^{-1} and 1342 cm^{-1} . The band at 1056 cm^{-1} (due to the ring oxygen) is shifted to 1088 cm^{-1} . The band at 882 cm^{-1} is shifted to 758 cm^{-1} . The results indicate that the carboxylate anion and the ring oxygen are responsible for the interaction between the extract and the metal surface.

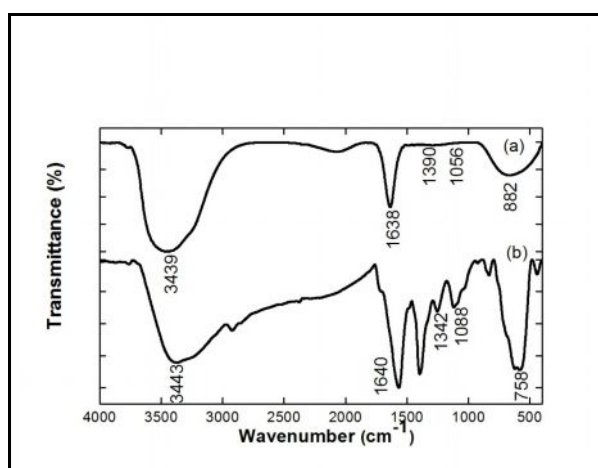


Fig. 5. FTIR Spectrum (KBr) (a) pure *Citrus medica* and (b) thin film formed on the surface of the carbon steel immersed in DD water containing *Citrus medica*

3.5. UV-vis study

The UV-Visible spectrum of Mn^{2+} , Fe^{2+} ion, *Citrus medica*, *Citrus medica*+ Mn^{2+} , and *Citrus medica* + Fe^{2+} ion in DD water are given in Figure 5.1.11a-e. The absorbance of *Citrus medica* at 240 nm is found to be 3.8908 (Fig. 5.1.11c). On increasing the λ , initially the absorbance decreases and reaches 3.8798 at 248.87 nm. The absorbance of Mn^{2+} ion is found to be 0.00260 at 338.11 nm and it decreases with increase in λ (Fig. 5.1.11a).

The addition of 20 ppm of Mn^{2+} to 300 ppm of *Citrus medica* increases the absorbance value. The absorbance is found to be 4.1285 at 231.92 nm and it decreases sharply to 318.96 nm (3.1170) (Fig. 5.1.11d). The higher value of absorbance in Mn^{2+} + *Citrus medica* constituent indicates the existence of strong interaction between Mn^{2+} and *Citrus medica*.

UV-visible spectrum of Fe^{2+} (Fig. 5.1.11b) shows that at 224 nm the solution has an absorbance of 0.12054. The absorbance decreases with increase in λ . A small peak is observed at 580 nm. When Fe^{2+} added to *Citrus medica* the absorbance is found to be 3.1070 at 198.96 nm (Fig. 5.1.11e) then decreases gradually upto 321.71 nm and then remains constant. This clearly proves the existence and formation of a complex between Fe^{2+} and *Citrus medica* [14,15].

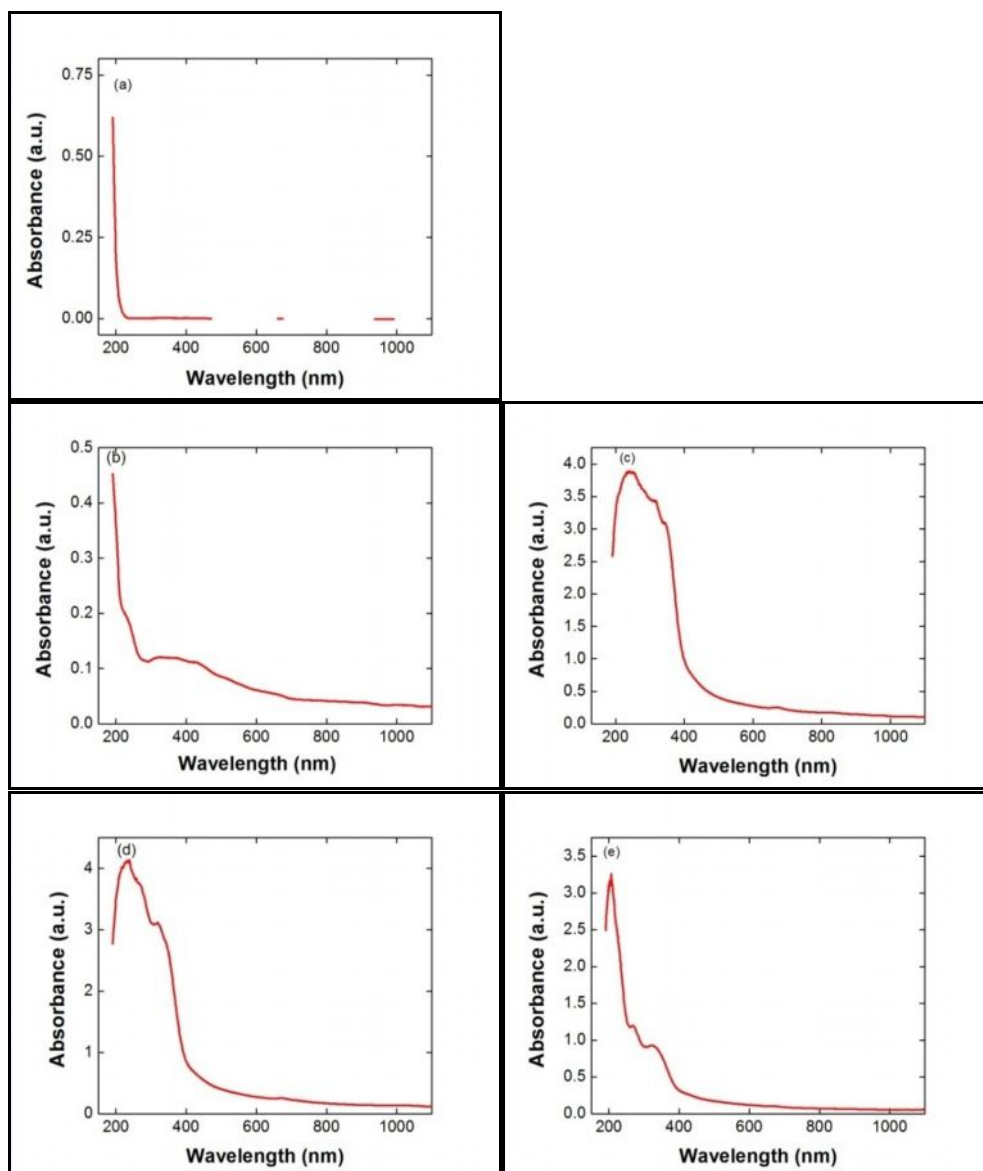


Fig. 6. UV-Visible absorption spectra of the test solutions in DD water (a) Mn^{2+} , (b) Fe^{2+} ion, (c) *Citrus medica*, (d) *Citrus medica*+ Mn^{2+} , and (e) *Citrus medica* + Fe^{2+}

4. Conclusion

The following conclusions were made from the following studies,

1. The corrosion rate of mild steel in DD water decreases with increase in concentration of CM.
2. The maximum inhibition efficiency of CM is found to be 81.58% at 300 ppm of inhibitor from mass loss studies.
3. Electrochemical measurements revealed that incorporation of CM significantly improved the inhibition performance, and produced strong synergistic inhibition effect.
4. All EIS spectra exhibit one capacitive loop which indicates that the electrochemical reaction is controlled by charge transfer process.
5. The FTIR spectrum confirms the formation of iron-CM complex.
6. The UV-visible absorption spectra, indicates the possibility of formation of iron-CM complex and Mn^{2+} -CM complex in the presence of inhibitor formulation.

References

1. P. Mourya, S. Banerjee, M.M. Singh, *Corr. Sci.* 85 (2014) 352.
2. W. Meier, *Chem. Soc. Rev.* 29 (2000) 295.

3. X. Lu, Z. Xin, *Colloid Polym. Sci.* 284 (2006) 1062.
4. D. Shchukin, H. Möhwald, *Adv. Funct. Mater.* 17 (2007) 1451.
5. A.M. Atta, G.A. El-Mahdy, H.A. Al-Lohedan, A.O. Ezzat, *Molecules* 19 (2014) 6246-6262.
6. N. Selvakumar, K. Jeyasubramanian, R. Sharmila, *Prog. Org. Coat.* 74 (2012) 461-469.
7. G. Schneider, G. Decher, *Nano Lett.* 4 (2004) 1833.
8. D.V. Andreeva, D. Fix, H. Möhwald, D.G. Shchukin, *J. Mater. Chem.* 18 (2008) 1738.
9. D. Shchukin, H. Möhwald, *Adv. Funct. Mater.* 17 (2007) 1451.
10. D.G. Shchukin, M. Zheludkevich, K. Yasakau, S. Lamaka, M.G.S. Ferreira, H. Möhwald, *Adv. Mat.* 18 (2006) 1672.
11. B. Leggat, W. Zhang, R. G. Buchheit, S. R. Taylor, *Corrosion*, 58 (2002) 322.
